

This is the accepted manuscript made available via CHORUS. The article has been published as:

## Second generation of “Miranda procedure” for CP violation in Dalitz studies of B (and D and $\tau$ ) decays

I. Bediaga, J. Miranda, A. C. dos Reis, I. I. Bigi, A. Gomes, J. M. Otalora Goicochea, and A. Veiga

Phys. Rev. D **86**, 036005 — Published 20 August 2012

DOI: [10.1103/PhysRevD.86.036005](https://doi.org/10.1103/PhysRevD.86.036005)

# Second Generation of ‘Miranda Procedure’ for CP Violation in Dalitz Studies of $B$ (& $D$ & $\tau$ ) Decays

I. Bediaga, J. Miranda, and A. C. dos Reis  
*Centro Brasileiro de Pesquisas Físicas*

I.I. Bigi  
*Department of Physics, University of Notre Dame du La*

A. Gomes and J. Otalora  
*Instituto de Física, Universidade Federal do Rio de Janeiro*

A. Veiga  
*Departamento de Energia Elétrica, Pontifícia Universidade Católica do Rio de Janeiro*

The ‘Miranda Procedure’ proposed for analyzing Dalitz plots for CP asymmetries in charged  $B$  and  $D$  decays in a model-independent manner is extended and refined. The complexity of CKM CP phenomenology through order  $\lambda^6$  is needed in searches for New Dynamics (ND). Detailed analyses of three-body final states offer great advantages: (i) They give us more powerful tools for deciding whether an observed CP asymmetry represents the manifestation of ND and its features. (ii) Many advantages can already be obtained by the ‘Miranda Procedure’ without construction of a detailed Dalitz plot description. (iii) One studies CP asymmetries independent of production asymmetries. We illustrate the power of a second generation Miranda Procedure with examples with time integrated rates for  $B_d/\bar{B}_d$  decays to final states  $K_S\pi^+\pi^-$  as trial runs with comments on  $B^\pm \rightarrow K^\pm\pi^+\pi^-/K^\pm K^+K^-$ .

PACS numbers: 11.30.Er

## I. LANDSCAPE OF $B_{u,d,s}$ , $D_{u,d,s}$ & $\tau$ CP VIOLATIONS

The predictions of CKM theory have been impressively confirmed to a degree that has persuaded a part of our community to focus on scenarios of Minimal Flavour Violation (MFV) – i.e., models of New Dynamics (ND) that contain the same sources of flavour violations as the Standard Model (SM). Some intriguing work has been done along these lines, yet we view the hypothesis of MFV as far from compelling at present. The data still allow for sizable deviations from SM predictions in heavy flavour transitions; in  $D^0$  and some  $B_s$  decays they could even be dominant. Furthermore, baryogenesis requires the intervention of ND with CP violation. If ND appears around the  $\mathcal{O}(1 \text{ TeV})$  scale underlying the weak-electric phase transition, which is not intrinsically connected with flavour dynamics, it will affect CP asymmetries in heavy flavour decays – but not on the leading level. CP asymmetries are given by three classes of observables, namely

- $|q/p| \neq 1$ , which shows purely indirect CP violation.
- Absolute amplitudes  $|A_f| \neq |\bar{A}_f|$  that show purely direct CP violation and depend on the final states.
- The relative phases between  $q/p$  and  $\bar{A}_f \otimes A_f^*$ , which will depend on the final state  $f$ . We write  $\bar{A}_f \otimes A_f^*$  rather than just  $\bar{A}_f A_f^*$ , because for a three-body final state one has to denote the position in the two-dimension plot. The significance of this feature will become clearer through the illustrations given below.

### A. Present Status of CP Asymmetries in $B$ , $D$ & $\tau$ Transitions

Oscillations have been observed for all three heavy flavours  $B_s$ ,  $B_d$  and  $D^0$  mesons, but on very different numerical levels.

#### 1. Indirect CP Violation in $B_{d,s}$ Transitions

Indirect CP violation has been measured with very good accuracy in  $B_d \rightarrow \psi K_S/K_L$  and  $B_d \rightarrow \pi^+\pi^-$  [1]:

$$S(B_d \rightarrow \psi K_S) = 0.658 \pm 0.024 \quad (1)$$

$$S(B_d \rightarrow \pi^+\pi^-) = -0.61 \pm 0.08 \quad (2)$$

Purely indirect CP violation gives  $S(B_d \rightarrow \psi K_S) = -S(B_d \rightarrow \pi^+\pi^-)$ .

Very recent data from LHCb [2] on  $B_s \rightarrow \psi\phi$ ,  $\psi f_0(980)$  give

$$\phi_s = -0.002 \pm 0.083 \pm 0.027 \text{ rad} \quad (3)$$

#### 2. Direct CP Violation in $B_{u,d,s}$ Transitions

Direct CP asymmetries has been established in  $B_d$  decays [1, 3]:

$$A_{CP}(B_d \rightarrow K^+\pi^-)|_{\text{PDG}'10} = -0.098 \pm 0.013 \quad (4)$$

$$A_{CP}(B_d \rightarrow K^+\pi^-)|_{\text{LHCb}'11} = -0.088 \pm 0.011 \pm 0.008 \quad (5)$$

$$C(B_d \rightarrow \pi^+\pi^-) = -0.38 \pm 0.17 \quad (6)$$

No sign for direct CP violation has been found in  $B_d \rightarrow K_S\pi^0$  – by sizable asymmetry can still be allowed:

$$A_{CP}(B_d \rightarrow K_S\pi^0)|_{\text{PDG}'10} = 0.00 \pm 0.13 \quad (7)$$

Intriguing evidences for direct CP violation has been found in  $B_s$  and  $B^+$  in (quasi-)two-body final states [1, 3, 4]:

$$A_{CP}(\bar{B}_s \rightarrow K^+\pi^-)|_{\text{LHCb}'11} = +0.27 \pm 0.08 \pm 0.02 \quad (8)$$

$$A_{CP}(B^+ \rightarrow D_{CP[+1]}K^+) = +0.24 \pm 0.06 \quad (9)$$

$$A_{CP}(B^+ \rightarrow \rho^0 K^+) = +0.37 \pm 0.10 \quad (10)$$

$$A_{CP}(B^+ \rightarrow f_0(1370)\pi^+) = +0.72 \pm 0.22 \quad (11)$$

$$A_{CP}(B^+ \rightarrow \eta K^+) = -0.37 \pm 0.09 \quad (12)$$

$$A_{CP}(B^+ \rightarrow f_2(1270)K^+) = -0.68^{+0.19}_{-0.17} \quad (13)$$

$$A_{CP}(\bar{B}_s \rightarrow K^+\pi^-)|_{\text{LHCb}'11} = +0.27 \pm 0.08 \pm 0.02 \quad (14)$$

$$A_{CP}(\bar{B}_s \rightarrow K^+\pi^-)|_{\text{CDF}} = +0.39 \pm 0.15 \pm 0.08 \quad (15)$$

### 3. Evidence for CP Asymmetries in $D^0$ Decays

No sign of indirect CP violation has been found in  $D^0 \rightarrow K^+K^-/\pi^+\pi^-$  [5]:

$$\left| \frac{q}{p} \right| = 0.88^{+0.18}_{-0.16}, \quad \phi = (-10.2^{+9.4}_{-8.9})^\circ \quad (16)$$

Direct CP asymmetry has been found in  $\Gamma(D^0 \rightarrow K^+K^-) - \Gamma(D^0 \rightarrow \pi^+\pi^-)$  with 3.5 sigma away from zero by LHCb [6] and with 2.7 sigma by CDF [7];

$$\Delta A_{CP} = -0.82 \pm 0.21(\text{stat}) \pm 0.11(\text{syst})\% \quad \text{LHCb} \quad (17)$$

$$\Delta A_{CP} = -0.62 \pm 0.21(\text{stat}) \pm 0.10(\text{syst})\% \quad \text{CDF} \quad (18)$$

with  $\Delta A_{CP} \equiv A_{CP}(D^0 \rightarrow K^+K^-) - A_{CP}(D^0 \rightarrow \pi^+\pi^-)$ . This is the first significant evidence for CP violation in  $\Delta C \neq 0$  dynamics, and it is important whether it is due to alone SM or need impact from ND.

### 4. Evidence for CP Asymmetries in $\tau$ Decays

In  $\tau^- \rightarrow K_S \pi^- \nu$  decays one has a prediction [8]

$$A_{CP}(\tau^+ \rightarrow \bar{\nu} + K_S \pi^+)|_{\text{SM}} = (0.36 \pm 0.01)\%, \quad (19)$$

independent of dynamics that generate  $K^0 \rightarrow \bar{K}^0$  oscillations, and data from the BaBar Collab. [9]:

$$A_{CP}(\tau^+ \rightarrow \bar{\nu} + K_S \pi^+[\geq 0 \pi^0])|_{\text{BaBar}} = (-0.36 \pm 0.23 \pm 0.11)\% . \quad (20)$$

## B. CKM Matrix Parametrization through $\mathcal{O}(\lambda^6)$

The usually applied the Wolfenstein parameterization of the CKM matrix gives real parts through  $\mathcal{O}(\lambda^3)$  and the imaginary part through  $\mathcal{O}(\lambda^4)$ . The CKM matrix is usually described by the four parameters  $\lambda$ ,  $\rho$ ,  $\eta$  and  $A$  with the last three ones of order unity; thus one gets  $|V_{ub}/V_{cb}| \simeq \lambda \sqrt{\rho^2 + \eta^2} \sim \mathcal{O}(\lambda)$ .

PDG states  $|V_{ub}/V_{cb}| \sim 0.085$ . The global fit leads to  $\rho \simeq 0.13$  and  $\eta \simeq 0.34$ . It means that one has to use a parametrization with through order of  $\lambda^6$  and with other quantities of true order of unity. One has been found in Ref.[10]:

$$\begin{pmatrix} 1 - \frac{\lambda^2}{2} - \frac{\lambda^4}{8} - \frac{\lambda^6}{16}, & \lambda, & \bar{h}\lambda^4 e^{-i\delta_{QM}}, \\ -\lambda + \frac{\lambda^3}{2}f^2, & 1 - \frac{\lambda^2}{2} - \frac{\lambda^4}{8}(1 + 4f^2) - f\bar{h}\lambda^5 e^{-i\delta_{QM}}, & f\lambda^2 + \bar{h}\lambda^3 e^{-i\delta_{QM}} \\ & + \frac{\lambda^6}{16}(4f^2 - 4\bar{h}^2 - 1), & -\frac{\lambda^5}{2}\bar{h}e^{-i\delta_{QM}}, \\ f\lambda^3, & -f\lambda^2 - \bar{h}\lambda^3 e^{-i\delta_{QM}}, & 1 - \frac{\lambda^4}{2}f^2 - f\bar{h}\lambda^5 e^{-i\delta_{QM}} \\ & + \frac{\lambda^4}{2}f + \frac{\lambda^6}{8}f, & -\frac{\lambda^6}{2}\bar{h}^2 \end{pmatrix} + \mathcal{O}(\lambda^7) \quad (21)$$

A global fit of the CKM matrix gives:  $\lambda \simeq 0.225$ ,  $f \simeq 0.75$ ,  $\bar{h} \simeq 1.35$  and the ‘maximal’ phase  $\delta_{QM} \simeq 90^\circ$ .

This pattern is not so obvious as from the Wolfenstein parametrization, more subtle for CP violation and is similar only in a semi-quantitative way [11]. To give three examples:

- CP asymmetry in  $B_d \rightarrow \psi K_S$  depends in SM on

$$-\text{Im} \frac{V_{tb}^* V_{td} V_{cb} V_{cs}^*}{V_{tb} V_{td}^* V_{cb}^* V_{cs}} \simeq \frac{\frac{2\bar{h}\lambda}{f} \sin\delta_{\text{QM}} + \left(\frac{\bar{h}\lambda}{f}\right)^2 \sin 2\delta_{\text{QM}}}{1 + \left(\frac{\bar{h}\lambda}{f}\right)^2 + \frac{2\bar{h}\lambda}{f} \cos\delta_{\text{QM}}} \quad (22)$$

One gets:

$$S(B_d \rightarrow \psi K_S) = \sin 2\phi_1 \simeq 0.63 - 0.69 \text{ for } \delta_{\text{QM}} \simeq 75^\circ - 90^\circ \quad (23)$$

$$S(B_d \rightarrow \psi K_S) = \sin 2\phi_1 \sim 0.74 \text{ for } \delta_{\text{QM}} \simeq 100^\circ - 120^\circ ; \quad (24)$$

i.e., CKM dynamics could produce  $S(B_d \rightarrow \psi K_S) \sim 0.74$  as largest value for CP asymmetry with  $\delta_{\text{QM}} \simeq 100^\circ - 120^\circ$ , not with the maximal  $\delta_{\text{QM}} = 90^\circ$ .

- Again one finds that indirect CP violation in  $B_s$  is CKM suppressed in the SM by

$$\text{Im} \left[ \frac{V_{tb}^* V_{ts} V_{cb} V_{cs}^*}{V_{tb} V_{ts}^* V_{cb}^* V_{cs}} \right] \simeq \frac{2(\bar{h}/f)\lambda^3 [\sin\delta_{\text{QM}} + 2(\bar{h}/f)\sin 2\delta_{\text{QM}}]}{1 + (4\bar{h}/f)\lambda \cos\delta_{\text{QM}}} \sim 0.03 - 0.05 . \quad (25)$$

with  $\delta_{\text{QM}} \simeq (75 - 120)^\circ$ .

- Direct CP violation in  $B^\pm \rightarrow D_\pm K^\pm$  depends on  $\sin\phi_3$ , where one gets:

$$\phi_3 = \arg \left( \frac{V_{ub}^* V_{ud}}{-V_{cb}^* V_{cd}} \right) \simeq (1 - \lambda^2/2) \frac{\bar{h}\lambda}{f} \frac{\sin\delta_{\text{QM}}}{1 + (\bar{h}\lambda/f)^2 + 2(\bar{h}\lambda/f)\cos\delta_{\text{QM}}} \quad (26)$$

Thus

$$\phi_3 = 0.28 / 0.34 / 0.42 \text{ for } \delta_{\text{QM}} = 75^\circ / 90^\circ / 110^\circ . \quad (27)$$

Therefore  $\sin 2\phi_1 \simeq 0.69 \pm 0.06$  and  $\sin\phi_3 \simeq 0.34 \pm 0.07$  are consistent with CKM dynamics with *lower* values of  $\phi_1$  &  $\phi_3$  correlated with each other with 10 % vs. 20 %. Nevertheless the impact of ND can ‘hide’ in predicted CP asymmetries.

### C. Present Resume on CP Asymmetries in Two-Body Final States in $B$ and $D$ Decays

SM generates indirect and direct CP asymmetries in  $B$  &  $D$  (and in  $K$ ) transitions. Their strengths are based on several items:

- The CKM matrix is discussed above in Sect.IB. We can say that SM is at least the leading source of CP violation in  $B$  on most transitions – except at present for  $B_s \rightarrow \psi\phi/\psi f_0(980)$ . On the other hand ND can affect CP asymmetries on the level of  $\sim 10 - 20\%$  for  $B_{u,d}$  decays. Furthermore one has to focus on correlations with CKM suppressed decays of  $B_{u,d,s}$  (and  $K$  and  $D_{(s)}$ ) on the level of 20 %. Therefore one need more accuracy from data and their interpretation to find impact of one (or two) ND – and to probe three-body final states.
- While the final states  $K^+\pi^-$  in  $B_d$  and  $\bar{B}_s$  are the same, the underlying dynamics are very different:
  - SM amplitudes for  $\bar{B}_d \rightarrow K^-\pi^+$  are given by ‘tree’ Cabibbo suppressed transitions  $b \rightarrow u\bar{u}s$  and (1-loop) ‘Penguin’  $b \rightarrow s\bar{q}q$ ;  $\sim 10\%$  CP asymmetry seems a reasonable value in SM.
  - On the other hand SM amplitude for  $\bar{B}_s \rightarrow K^+\pi^-$  is given by ‘tree’ Cabibbo favoured  $b \rightarrow u\bar{u}d$  and Cabibbo suppressed ‘Penguin’  $b \rightarrow d\bar{q}q$ . Therefore one expects CP asymmetry on the ‘natural’ level of  $\mathcal{O}(1\%)$ .  
ND can enhance ‘Penguin’ amplitude significantly. However one expects such effect in other  $B$  decays – unless a nearby resonance can affect mostly  $B_s$ , but not  $B_{d,u}$  decays.

For  $D$  decays the landscape is much more subtle, but also very ‘topical’:

- CKM dynamics produce direct CP asymmetries in singly Cabibbo suppressed (SCS) decays around the scale of 0.001.

– CP asymmetries in double Cabibbo suppressed (DCS) ones are zero at  $\mathcal{O}(\lambda^4)$ .

- CP asymmetries are controlled by non-perturbative QCD.
- The difference between  $A_{\text{CP}}(\tau^+ \rightarrow \bar{\nu} + K_S \pi^+ [\geq 0 \pi^0])|_{\text{measured}}$  and  $A_{\text{CP}}(\tau^+ \rightarrow \bar{\nu} + K_S \pi^+)|_{\text{SM}}$  depend on our control of non-perturbative QCD – like the plots of the final states of  $A_{\text{CP}}(\tau^+ \rightarrow \bar{\nu} + [K\pi]^+)$  and  $A_{\text{CP}}(\tau^+ \rightarrow \bar{\nu} + [K\pi\pi]^+)$  [12].

Finding impact of ND in CP asymmetries in  $B$  and  $D$  decays is one thing – however probing the ‘shape’ of one (or two) ND is another challenge.

Dedicated studies of three-bodies final states are needed to identify important features of ND involved [13]. Three-body final states analyses are very time consuming. In Sect.II we list the general advantages that such analyses merit the needed work; we first sketch in Sect.III the situations for three-body decays of  $B_s$ ,  $B_d$ ,  $D^0$  in general for searching CP asymmetries through (partly) time integrated data to set the stage; afterwards we give more realistic situations in  $B_d$  transitions in Sect.IV B and comments on  $B_s$  transitions in Sect.V; finally we summarize our main conclusions in Sect.VI.

## II. ADVANTAGES OF STUDIES OF THREE-BODY FINAL STATES

While the weak dynamics from CKM and ND are the driving forces for CP asymmetries, one has to control FSI from non-perturbative QCD not only in a qualitatively way – that is the focus of our study.

### A. Opportunities Offered by Dalitz Plot Studies

No study of any three-body final states in  $B$  decays have found an established CP violation, and none from  $K$  or  $D$  mesons shows any sign for it. However there can be – actually they are more likely to be found. *The average over CP asymmetries in a Dalitz plot is expected to be much larger than ‘local’ asymmetries, which often compensate with each other.* As explained in some detail in [13], crucial insights into CP odd dynamics will be learnt from their impact on final state distributions. Dalitz studies will play a central role in the future for several reasons:

- Differential or ‘local’ asymmetries could be considerably larger than ones averaged over the Dalitz plot.
- For two-body final states there is only one CP asymmetry, namely  $\Gamma(B^0/D^0 \rightarrow h^+ h^-)$  vs.  $\Gamma(\bar{B}^0/\bar{D}^0 \rightarrow h^+ h^-)$ . On the other hand the topologies of Dalitz plots for  $B^0 \rightarrow h^+ h^- h^0$  and  $\bar{B}^0 \rightarrow h^+ h^- h^0$  are in general different; for example the two half of the plots  $s_{h^+ h^0} - s_{h^- h^0}$  for the  $B^0$  and  $\bar{B}^0$  are different. *However their sum have to be symmetric – unless CP asymmetries occur!*
- While the difference in total rates for  $B/D \rightarrow 3h$  vs.  $\bar{B}/\bar{D} \rightarrow 3h$  are affected by production asymmetries, differences between corresponding regions in the Dalitz plots are not.
- Nontrivial correlations provide powerful validation tools.
- The pattern of a CP asymmetry that has emerged in a Dalitz plot can tell us about the spin structure of the underlying effective operator.
- The cleanest experimental sign whether an observed asymmetry is produced by direct or indirect CP violation (or which parts are due to one or the other) is their dependence on the time of decay. Direct asymmetry is independent of the time of decay, whereas indirect violation evolves in time in a clear prescription, since it is driven by oscillations. With only time integrated data with two-body final states one cannot decide it. If one observes a CP asymmetry in a leading CKM final state – like  $B_d \rightarrow \psi K_S$  or  $B_s \rightarrow \psi \phi$  – you will argue that it is most likely indirect. Yet for CKM-suppressed decays you hardly have such an argument. As explained later, one can use more decision criterions from three-body final states.
- Time *depending* CP asymmetries give us more informations about underlying dynamics for  $B^0$  and  $D^0$  transitions. Of course one needs more statistics. *Partially time integrated* rates for three-body final states give us more insights.

Dalitz studies offer also a more technical advantage when searching for CP asymmetries, namely ‘tunable’ strong phases. Since that is of direct relevance for our subsequent analysis, we explain it next.

## B. Phases with Breit-Wigner Resonances

With CP violation being expressed by a complex weak phase due to CPT invariance, it can lead to an observable asymmetry only if one has the interference between two different amplitudes. Yet more is needed: hadronization has to affect the two amplitudes differently. This is usually expressed by stating that the two amplitudes have to exhibit *different weak as well as strong* phases.

Consider the decay  $P \rightarrow f$  receiving contributions from two coherent amplitudes,

$$A(P \rightarrow f) = e^{i\phi_1^W} e^{i\delta_1^{\text{FSI}}} |\mathcal{A}_1| + e^{i\phi_2^W} e^{i\delta_2^{\text{FSI}}} |\mathcal{A}_2| \quad (28)$$

$$A(\bar{P} \rightarrow \bar{f}) = e^{-i\phi_1^W} e^{i\delta_1^{\text{FSI}}} |\mathcal{A}_1| + e^{-i\phi_2^W} e^{i\delta_2^{\text{FSI}}} |\mathcal{A}_2|, \quad (29)$$

where  $\phi_i^W$  and  $\delta_i^{\text{FSI}}$  are the weak and strong phases, respectively, and  $\mathcal{A}_i$  are the moduli of the amplitudes. The CP asymmetry between partial widths

$$A_{\text{CP}} = \frac{\Gamma(P \rightarrow f) - \Gamma(\bar{P} \rightarrow \bar{f})}{\Gamma(P \rightarrow f) + \Gamma(\bar{P} \rightarrow \bar{f})}, \quad (30)$$

is given by

$$A_{\text{CP}} = \frac{2 \sin(\Delta\phi^W) \sin(\Delta\delta^{\text{FSI}}) |\mathcal{A}_2 \mathcal{A}_1|}{1 + |\mathcal{A}_2 \mathcal{A}_1|^2 + 2 |\mathcal{A}_2 \mathcal{A}_1| \cos(\Delta\phi^W) \cos(\Delta\delta^{\text{FSI}})} \quad (31)$$

CP violation is induced by  $\Delta\phi^W$ , but it becomes observable only if the final state interaction (FSI) introduces a non-trivial phase shift.

For two-body final states it is often implied that the strong phases  $\delta_i^{\text{FSI}}$  carry a *fixed* value for a given final state  $f$  (the two amplitudes are assumed to have different isospin contents up to isospin violation).

In the case of three-body decays, the transition  $P \rightarrow f$  is dominated by resonant intermediate states. The requirement of non-trivial strong phase different is satisfied by the energy dependent phases of the resonances. The Breit-Wigner excitation curve for a resonance  $R$  reads

$$F_R^{\text{BW}}(s) = \frac{1}{m_R^2 - s - im_R \Gamma_R(s)}, \quad (32)$$

introducing a sizable phase as expressed through

$$\text{Im} F_R^{\text{BW}}(s) = \frac{m_R \Gamma_R(s)}{(m_R^2 - s)^2 + (m_R \Gamma_R(s))^2}, \quad (33)$$

where  $\Gamma_R(s)$  denotes the energy dependent relativistic width.

For  $P \rightarrow p_1 p_2 p_3$  we define  $s_1 = (p_1 + p_2)^2$  and  $s_2 = (p_1 + p_3)^2$ . The previously constant strong phases and amplitude moduli in Eq.(31) now depend on the position in the Dalitz plot,  $\delta^{\text{FSI}} \rightarrow \delta(s_1, s_2)$  and  $\mathcal{A} \rightarrow \mathcal{A}(s_1, s_2)$ . The resonant amplitudes populate the whole phase space in  $D$  decays, and a large portion of it in  $B$  decays. Therefore, the CP asymmetry will also depend on the Dalitz plot coordinates,  $A_{\text{CP}} \rightarrow A_{\text{CP}}(s_1, s_2)$ .

After taking the modulus square of these amplitudes one reads off that a CP asymmetry will arise, when there are non-zero *weak* phases. Having to deal with non-uniform strong phases might appear as a complication that just creates more work for analysis of decays with three-(and four-)body final states. However there is an award for extra works: a resonance – in particular if it is relatively narrow – can tell us where CP asymmetries have to be and that the asymmetry has to change over a relatively narrow range in the Dalitz plot. The Dalitz plots carry the same area independent of production asymmetries; yet the *relative corresponding population densities* probe CP invariance.

## C. ‘Miranda Procedure’

*Indirect* CP violation in  $B^0$  decays is and will be well measured in  $B_d \rightarrow \psi K_S$  and  $B_s \rightarrow \psi \phi, \psi f_0(980)$  – and maybe in  $D^0 \rightarrow \phi K_S$ ; ND can impact those transitions in a sizable way. *Direct* CP violations affect final states in different strengths, in particular CKM suppressed ones both in SM and ND. The *existence* of ND might – and probably will – be found in indirect and direct CP violation in two-body final states – yet its main *features* have to be extracted from three-(and four-)body final states. Some asymmetries can tell us about the spin operators creating about etc. There are three classes of sources of CP asymmetries, namely

1. from CP conjugated quasi-two-body final states;
2. interference between quasi-two-body final states;
3. contributions from "true" three-body final states or broad resonances like  $\sigma$ .

Contributions from the first class like  $K\rho$  or  $\pi\rho$  are obvious. However from the second class one finds positive and negative contributions to the CP asymmetry; therefore those get washed out from the total integral over the phase space. This applies mostly to the third class of CP asymmetries. Therefore we will denote CP asymmetries from the first and second classes by  $CPV_A$  and  $CPV_I$  below. For the third class one can help sizably from future theoretical efforts.

The advantages listed above for CP studies in three-body final states justify the considerable ‘overhead’ in statistics and tuning efforts that constructing a satisfactory Dalitz model requires. Yet one *cannot count* on obtaining a *unique* Dalitz model even with infinite statistics. It is thus of considerable practical value to develop another method for analyzing a Dalitz plot that is model-independent; it will allow important statements about the existence of a CP asymmetry and its approximate localization inside the Dalitz plot with smaller data sets than constructing a full fledged Dalitz model. At the very least it would help to identify the sub-domain in the Dalitz plot where one had to focus the tuning efforts for the Dalitz model.

In Ref. [13] we have proposed one method that can serve such a purpose in a quantifying way. When searching for CP asymmetries we have suggested to analyze the *significance*

$$\Sigma(i) \equiv \frac{N(i) - \bar{N}(i)}{\sqrt{N(i) + \bar{N}(i)}}, \quad (34)$$

which amounts to a standard deviation for a Poissonian distribution rather than the customary *fractional* asymmetry

$$\Delta(i) \equiv \frac{N(i) - \bar{N}(i)}{N(i) + \bar{N}(i)} \quad (35)$$

in particle vs. anti-particle populations  $N(i)$  and  $\bar{N}(i)$  for each bin  $i$ , respectively. One analyzes, whether the  $\Sigma(i)$  distribution has a higher frequency of exhibiting large deviations from zero than expected for fluctuations. We have illustrated this method – ‘mirandizing’ in vernacular – by applying it to  $B^\pm \rightarrow K^\pm \pi^+ \pi^-$  and  $D^\pm \rightarrow \pi^\pm \pi^+ \pi^-$ ; the Dalitz plots have been constructed with fast MC simulations making specific assumptions about the underlying dynamics and the source of the CP asymmetry. In those pilot studies we could show that using the observable  $\Sigma(i)$  instead of  $\Delta(i)$  allowed a much more robust extraction of the seeded CP asymmetry and its location inside the Dalitz plot. It remains to be seen of course how mirandizing holds up when treating real data.

Our claim is *not* to replace full fledged Dalitz plot analysis. Our goal is to present an analysis that can produce significant results on CP violations from smaller data set while maintaining many of the advantages of a full Dalitz plot study. The latter is still the final goal of our road to ‘Rome’ – the impact of New Physics on CP violations in nonleptonic decays of beauty and charm hadrons. We also want to encourage others to try other possible roads to this ‘Rome’. An interesting work can be found in Ref. [14]

#### D. Comment on CP Asymmetries in $\tau^- \rightarrow \nu[K\pi/K\pi\pi]^-$

The SM generates a global CP asymmetries in  $\tau^- \rightarrow \nu K_S[S=0]$  due to  $K^0 - \bar{K}^0$  oscillations with  $2\text{Re } \epsilon_K$ , but not beyond that. On the other hand ND has a larger chance to appear in the CP asymmetries in  $\tau^- \rightarrow \nu[K\pi's]^-$ , since SM amplitudes are Cabibbo suppressed.

For  $\tau^- \rightarrow \nu[K\pi]^-$  one has a three-body final states in general, and in  $\tau^- \rightarrow \nu[K2\pi/3K]^-$  one has three-body hadronic final states. The ‘Miranda Procedure’ can and should be applied here with some refining Dalitz plots: the masses of the hadronic systems are not fixed as in  $B$  and  $D$  decays.

### III. SETTING THE STAGE FOR PROBING CP INVARIANCE

Both indirect and directly CP violations have been established in  $K^0$  and  $B_d$  transitions, and SM through CKM theory gives at least the leading contributions. The ND expected – or hoped for – to find around the few TeV scales should produce some ‘footprints’ through CP asymmetries in  $B$  and  $D$  transitions. However ‘reading’ them produces large both experimental and theoretical challenges. The time evolutions of the flavour tagged transitions provide the



most powerful tool in identifying to source of the underlying dynamics. To begin this projects we want to show what you learn from *non-flavour tagging* transitions *without* time resolved analyses.

For this study we describe the time integrated rates also for non-flavour tagged data and give comments on partly time resolved rates.

CP asymmetries are control by five observables:

1.  $x = \Delta M/\bar{\Gamma}$  and  $y = \Delta\Gamma/2\bar{\Gamma}$ , which are insensitive to CP violation;
2.  $|q/p| \neq 1$ , which shows purely indirect CP violation, and is determined by  $|q/p| \simeq 1 - \frac{1}{2}a_{SL}^{\text{CP}}$ , where denote the CP asymmetry in semi-leptonic decays in ‘wrong’-sign leptons;
3. absolute amplitudes  $|A_f| \neq |\bar{A}_f|$  that show purely direct CP violation and depend on the final states and
4. the relative phases between  $q/p$  and  $\bar{A}_f \otimes A_f^*$ , which will depend on the final state  $f$  due to direct CP violation. We write  $\bar{A}_f \otimes A_f^*$  rather than just  $\bar{A}_f A_f^*$ , because for a three-body final state one has to denote the position in the two-dimension plot. The significance of this feature will become clearer through the our illustrations later.

We give general expressions with these observables. Then we show that in describing for  $B_d$  decays we can ignore  $y_d$  effects, while for  $D^0$  decays one has to include both  $x_D$  and  $y_D$  dependences, but only to first order. For  $B_s$  transitions one has  $x_s \gg y_s$ , but one has to include  $y_s$  effects due to spectacularly fast  $x_s$  oscillations for time integrated data; CP asymmetries controlled by  $\text{Im}_{p_s}^{q_s} \bar{A}_f \otimes A_f$  are suppressed by  $1/x_s$ .

Indirect CP violation affects all channels through two quantities, namely  $|q/p|$  and the relative phase between  $q/p$  and  $\bar{A}_f \otimes A_f^*$ ; their weight of course depends on  $||q/p| - 1|$  and the strength of  $|\bar{A}_f \otimes A_f^*|$ . As mentioned above we can use the approximation of  $|q/p| = 1$  for  $B_d$  and  $B_s$  channels; the effect of indirect CP violation is affected the direct CP on rate  $B_d$  and  $B_s$  modes and therefore the impact of ND that is probably different for mode to mode.

For two-body final states like  $B_s \rightarrow h^+ h^-$  vs.  $\bar{B}_s \rightarrow h^+ h^-$  time dependent CP asymmetries are reduced by  $1/x_s^2$ ; however for direct CP violation in  $B_s \rightarrow h^+ h^- h^0$  vs.  $\bar{B}_s \rightarrow h^+ h^- h^0$  one can find an asymmetry between corresponding regions of the *sum of Dalitz plots of  $B_s \rightarrow f$  and  $\bar{B}_s \rightarrow f$  due to interference effects* – i.e., *without* flavour tagging.

Obviously flavour tagged time resolved analyses bring the largest information about the underlying dynamics; our main goal for this study is how many lessons can be obtained from non-flavour tagged time integrated data. Flavour-tagged and time resolved data will come later.

### A. Three-Body Decays for Neutral Mesons

For neutral  $B$  or  $D$  decays into two-body final states like  $K^+ K^-$  or  $\pi^+ \pi^-$ , it is clear that it is a (even) CP eigenstate. For  $f = h^+ h^- h^0$  like  $K_S \pi^+ \pi^-$ ,  $K_S K^+ K^-$  or  $\pi^+ \pi^- \pi^0$  the judgement is more complex: it can be [CP=+]  $K_S f_0(980)/K_S \sigma \rightarrow K_S \pi^+ \pi^-$ , [CP=-]  $K_S \phi \rightarrow K_S K^+ K^-$ , [CP=-]  $\rho^0 \pi^0 \rightarrow \pi^+ \pi^- \pi^0$  or [CP=+]  $\sigma \pi^0 \rightarrow \pi^+ \pi^- \pi^0$ . At the same time one has final states  $K^{*\pm} \pi^\mp$ ,  $\rho^\pm \pi^\mp$  etc. and interferences between them. Not only the total time integrated widths for  $P \rightarrow h^+ h^- h^0$  vs.  $\bar{P} \rightarrow h^+ h^- h^0$  give us a lesson on CP violating dynamics, but also their ‘topologies’ – i.e., the distributions over the Dalitz plots. Therefore we denote  $A_f$  and  $\bar{A}_{\bar{f}}$  for  $P \rightarrow h^+ h^- h^0$  and  $\bar{P} \rightarrow h^+ h^- h^0$ , respectively.

The ‘Miranda procedure’ can be applied to all three-body final states, but here we will discuss it only for  $f = h^+ h^- h^0$  like  $K_S \pi^+ \pi^-$ .

The *time dependent* rates can distinguish the three types of CP violations:  $|q/p| \neq |p/q|$ ,  $|A_f| \neq |\bar{A}_{\bar{f}}|$  and  $\text{Im}_p^q \bar{A}_f \otimes A_f^* \neq \text{Im}_q^p A_f \otimes \bar{A}_{\bar{f}}^*$ . For practical reasons we focus on *time integrated* widths for this study:

$$\Gamma(P \rightarrow f) = \frac{C}{\Gamma_1} \left[ a + \frac{1}{1 - \frac{\Delta\Gamma}{\Gamma_1}} b + \frac{1}{1 - \frac{\Delta\Gamma}{2\Gamma_1}} \frac{1}{1 + \frac{(\Delta M)^2}{(\Gamma_1 - \frac{\Delta\Gamma}{2})^2}} \left[ c + \frac{\Delta M}{\Gamma_1 - \frac{\Delta\Gamma}{2}} d \right] \right] \quad (36)$$

$$\Gamma(\bar{P} \rightarrow \bar{f}) = \frac{C}{\Gamma_1} \left[ \bar{a} + \frac{1}{1 - \frac{\Delta\Gamma}{\Gamma_1}} \bar{b} + \frac{1}{1 - \frac{\Delta\Gamma}{2\Gamma_1}} \frac{1}{1 + \frac{(\Delta M)^2}{(\Gamma_1 - \frac{\Delta\Gamma}{2})^2}} \left[ \bar{c} + \frac{\Delta M}{\Gamma_1 - \frac{\Delta\Gamma}{2}} \bar{d} \right] \right] \quad (37)$$

CP violation can appear in the *time integrated* widths in principle from the three sources listed above.

While the *time integrated* observables have the largest statistics, the *time dependent* ones have most detailed information about the underlying dynamics; *partially* integrated one can give us most of that information depending

on how the parameters for the hadrons and their transitions.

$$\Gamma_t^\infty \equiv \int_t^\infty dt \Gamma(P \rightarrow f; t) \quad (38)$$

$$\bar{\Gamma}_t^\infty \equiv \int_t^\infty dt \Gamma(\bar{P} \rightarrow \bar{f}; t); \quad (39)$$

therefore

$$\Gamma_0^t = \Gamma(P \rightarrow f) - \Gamma_t^\infty \quad (40)$$

$$\bar{\Gamma}_0^t = \Gamma(\bar{P} \rightarrow \bar{f}) - \bar{\Gamma}_t^\infty \quad (41)$$

### 1. $B_d \rightarrow h^+ h^- h^0$

For  $B_d$  transitions one can simplify these expressions in two ways, namely  $y_d \simeq 0$  and  $|q_d/p_d| \simeq 1$  for realistic experimental sensitivities. Integrated over *all times of decays* we get

$$\int_0^\infty dt |\mathcal{A}(B_d \rightarrow f; t)|^2 = \frac{C}{\Gamma_{B_d}} \left[ |A_f|^2 + |\bar{A}_{\bar{f}}|^2 + \frac{1}{1+x_d^2} (|A_f|^2 - |\bar{A}_{\bar{f}}|^2) - \frac{2x_d}{1+x_d^2} \text{Im} \left( \frac{q_d}{p_d} \bar{A}_{\bar{f}} \otimes A_f^* \right) \right] \quad (42)$$

$$\int_0^\infty dt |\mathcal{A}(\bar{B}_d \rightarrow \bar{f}; t)|^2 = \frac{C}{\Gamma_{B_d}} \left[ |A_f|^2 + |\bar{A}_{\bar{f}}|^2 + \frac{1}{1+x_d^2} (|\bar{A}_{\bar{f}}|^2 - |A_f|^2) + \frac{2x_d}{1+x_d^2} \text{Im} \left( \frac{q_d}{p_d} \bar{A}_{\bar{f}} \otimes A_f^* \right) \right] \quad (43)$$

For equal productions of  $B_d$  and  $\bar{B}_d$  -  $\rho(B_d) = \frac{1}{2} = \rho(\bar{B}_d)$  - we get

$$\frac{1}{2} \left[ \int_0^\infty dt |\mathcal{A}(B_d \rightarrow f; t)|^2 + \int_0^\infty dt |\mathcal{A}(\bar{B}_d \rightarrow \bar{f}; t)|^2 \right] = |A_f|^2 + |\bar{A}_{\bar{f}}|^2 \quad (44)$$

For a two-body final state  $f = h^+ h^-$  one gets no information about CP violation from the time integrated sum as expected. However for  $f = h^+ h^- h^0$  direct CP violation can produce an asymmetry in *corresponding* regions of the *sum of Dalitz plots* as sketched before. Our studies given below will illustrate this feature. Their sum is weighted by their ratio due to a real production asymmetry (or a difference in their efficiencies)

$$\rho(B_d) \int_0^\infty dt |\mathcal{A}(B_d \rightarrow f; t)|^2 + (1 - \rho(B_d)) \int_0^\infty dt |\mathcal{A}(\bar{B}_d \rightarrow \bar{f}; t)|^2 = \frac{1}{1+x_d^2} \left[ (2\rho(B_d) + x_d^2) |A_f|^2 + (2(1 - \rho(B_d)) + x_d^2) |\bar{A}_{\bar{f}}|^2 + 2x_d(1 - 2\rho(B_d)) \text{Im} \left( \frac{q_d}{p_d} \bar{A}_{\bar{f}} \otimes A_f^* \right) \right] \quad (45)$$

If there is *production asymmetry*, it is not a ‘vice’, but a ‘virtue’. It can be tracked by  $\bar{B}_d \rightarrow \psi K^- \pi^+$  vs.  $B_d \rightarrow \psi K^+ \pi^-$  or by  $B^\pm \rightarrow \psi K^\pm$ . The strength of indirect CP violation is measured in  $B_d \rightarrow \psi K_S$ , whether the SM produces the whole or just the leading source of it. Used as an *input* for  $B_d \rightarrow K_S \pi^+ \pi^-$ ,  $K_S K^+ K^-$  one can interpret the impact of direct CP violation through the term  $\text{Im} \left( \frac{q_d}{p_d} \bar{A}_{\bar{f}} \otimes A_f^* \right)$ , see Eq.(45).

### 2. $B_s \rightarrow h^+ h^- h^0$

For  $B_s$  transitions, one can assume  $|q_s/p_s| \simeq 1$ , since even with sizable ND contributions to  $B_s - \bar{B}_s$   $|q_s/p_s|$  can differ from unity not more than several permil. While  $\Delta\Gamma_s$  is small -  $y_s = \Delta\Gamma_s/2\bar{\Gamma}_s \simeq 0.094 \pm 0.024$  - it should not be ignored. Integrated over all times of decays we get

$$\int_0^\infty dt |\mathcal{A}(B_s \rightarrow f; t)|^2 \propto \frac{1}{2\Gamma_1} \cdot \left[ |A_f|^2 + |\bar{A}_{\bar{f}}|^2 + \frac{\Delta\Gamma_s}{\Gamma_1} \left( \frac{1}{2} (|A_f|^2 + |\bar{A}_{\bar{f}}|^2) - \text{Re} \left( \frac{q_s}{p_s} \bar{A}_{\bar{f}} \otimes A_f^* \right) \right) - \frac{2}{x_s} \text{Im} \left( \frac{q}{p} \bar{A}_{\bar{f}} \otimes A_f^* \right) + \mathcal{O}(1/x_s^2) \right] \quad (46)$$

$$\int_0^\infty dt |\mathcal{A}(\bar{B}_s \rightarrow \bar{f}; t)|^2 \propto \frac{1}{2\Gamma_1} \cdot \left[ |A_f|^2 + |\bar{A}_{\bar{f}}|^2 + \frac{\Delta\Gamma_s}{\Gamma_1} \left( \frac{1}{2} (|A_f|^2 + |\bar{A}_{\bar{f}}|^2) - \text{Re} \left( \frac{q_s}{p_s} \bar{A}_{\bar{f}} \otimes A_f^* \right) \right) + \frac{2}{x_s} \text{Im} \left( \frac{q}{p} \bar{A}_{\bar{f}} \otimes A_f^* \right) + \mathcal{O}(1/x_s^2) \right] \quad (47)$$

Therefore we get for non-flavour tagged sum

$$\begin{aligned} \Gamma_1 \left[ \int_0^\infty dt |\mathcal{A}(B_s \rightarrow f; t)|^2 + \int_0^\infty dt |\mathcal{A}(\bar{B}_s \rightarrow \bar{f}; t)|^2 \right] = \\ = 2|A_f|^2 + 2|\bar{A}_{\bar{f}}|^2 + 2y_s \left( (|A_f|^2 + |\bar{A}_{\bar{f}}|^2) - 2\text{Re} \left( \frac{q_s}{p_s} \bar{A}_{\bar{f}} \otimes A_f^* \right) \right) \end{aligned} \quad (48)$$

If there is a production asymmetry one gets:

$$\begin{aligned} \Gamma_1 \left[ \int_0^\infty dt |\mathcal{A}(B_s \rightarrow f; t)|^2 + \int_0^\infty dt |\mathcal{A}(\bar{B}_s \rightarrow \bar{f}; t)|^2 \right] = \\ = 2|A_f|^2 + 2|\bar{A}_{\bar{f}}|^2 + 2y_s \left( (|A_f|^2 + |\bar{A}_{\bar{f}}|^2) - 2\text{Re} \left( \frac{q_s}{p_s} \bar{A}_{\bar{f}} \otimes A_f^* \right) \right) + \frac{2(1 - 2\rho(B_s))}{x_s} \text{Im} \left( \frac{q}{p} \bar{A}_{\bar{f}} \otimes A_f^* \right) \end{aligned} \quad (49)$$

While the strength of indirect CP violation has not measured in time-resolved data on  $B_s \rightarrow \psi\phi$ , there are some evidence that it might be significantly larger than the CKM prediction of around  $\sin 2\beta_s \sim 0.03 - 0.05$ . That situation should be more clarified in one to three years. The  $2y_s$  term can give us useful information about the dynamics of  $B$  decays, but itself does not represent a CP asymmetry. In principal if there is a production asymmetry – it could be tracked by the Cabibbo suppressed transition  $\bar{B}_s \rightarrow \psi K^+ \pi^-$  vs.  $B_s \rightarrow \psi K^- \pi^+$  – one could obtain  $\text{Im} \left( \frac{q_s}{p_s} \bar{A}_{\bar{f}} \otimes A_f^* \right)$ ; however it is greatly suppressed in  $B_s \rightarrow K_S \pi^+ \pi^-$ ,  $K_S K^+ K^-$  by  $1/x_s$  – i.e., the spectacularly fast oscillation.

### 3. Comments on $B^0$ transitions

Our goal for  $B^0$  transitions is to analyse the impact of ND on *direct* CP asymmetries in *three-body* decays in CKM suppressed channels.

Indirect CP violation affects all transitions of a *given* meson –  $B_d$ ,  $B_s$  and  $D^0$  – in the same way. For  $B_d$  we have measured it with good accuracy in  $B_d \rightarrow \psi K_S$  with CKM dynamics as the leading source. The SM prediction tell us that  $|q_d/p_d|$  can differ from unity by less than 0.001.

For  $B_s$  transitions some evidence has been found in  $B_s \rightarrow \psi\phi$  and  $B_s \rightarrow l^- X$  processes for a large impact of ND. We expect that evidence will be validated or reject with good accuracy in the foreseeable future from LHCb, CMS and ATLAS. For the time being one can use two scenarios, namely

- Case CKM:  $\sin 2\beta_s \sim 0.03 - 0.05$ ,  $||q_s/p_s| - 1| < 0.0001$ ;
- Case CKM + ND:  $\sin 2\beta_s \simeq 0.11 \pm 0.02$ ,  $||q_s/p_s| - 1| \simeq 0.003$

keeping in mind that such cases will be decided about future data on  $B_s \rightarrow \psi\phi$  and  $B_s \rightarrow l^- DX$ . We consider the impact of ND in  $B_s \rightarrow K_S K^+ K^-$ ,  $K_S \pi^+ \pi^-$ .

### 4. $D^0 \rightarrow h^+ h^- h^0$

For  $D^0$  transitions both  $x_D$  and  $y_D$  are small and probably of similar size, but  $|q_D/p_D|$  could differ from unity by up to 30 %. Integrating over all times  $t$  of  $D^0$  decays one gets

$$\begin{aligned} \int_0^\infty dt |\mathcal{A}(D^0 \rightarrow f; t)|^2 + \int_0^\infty dt |\mathcal{A}(\bar{D}^0 \rightarrow \bar{f}; t)|^2 \propto \\ |A_f|^2 + |\bar{A}_{\bar{f}}|^2 - y_D \text{Re} \left( \frac{q}{p} + \frac{p^*}{q^*} \right) \bar{A}_{\bar{f}} \otimes A_f^* + x_D \text{Im} \left( \frac{q}{p} - \frac{p^*}{q^*} \right) \bar{A}_{\bar{f}} \otimes A_f^* \end{aligned} \quad (50)$$

An production asymmetry leads to

$$\begin{aligned} \rho(D^0) \int_0^\infty dt |\mathcal{A}(D^0 \rightarrow f; t)|^2 + (1 - \rho(D^0)) \int_0^\infty dt |\mathcal{A}(\bar{D}^0 \rightarrow \bar{f}; t)|^2 \propto \\ \rho(D^0) |A_f|^2 + (1 - \rho(D^0)) |\bar{A}_{\bar{f}}|^2 - y_D \text{Re} \left[ \left( \rho(D^0) \frac{q}{p} + (1 - \rho(D^0)) \frac{p^*}{q^*} \right) \bar{A}_{\bar{f}} \otimes A_f^* \right] + \\ + x_D \text{Im} \left[ \left( \rho(D^0) \frac{q}{p} - (1 - \rho(D^0)) \frac{p^*}{q^*} \right) \bar{A}_{\bar{f}} \otimes A_f^* \right] \end{aligned} \quad (51)$$

In  $D^0$  decays the interplay of indirect and direct CP violations is not so clear mostly due to very slow oscillation. Therefore we will consider scenarios with  $||q_D/p_D| - 1| \simeq 0.1, 0.03$ ,  $|A_f|/|\bar{A}_f| \simeq 0.1, 0.03$  and the relative phase of  $q_D/p_D$  and  $\bar{A}_f \otimes A_f^*$ . We will present studies in a future paper.

### 5. Comments on ND scenarios

For analyzing CP asymmetries in  $h^+h^-h^0$  final states one has to include not only  $PV$  final states, but also  $SP$  final states like scalar  $\sigma$  and  $\kappa$  resonances. One reason for that is that exchanges from charged Higgs fields will introduce CP asymmetries already on the zero-loop processes, and they will affect scalar resonances more than  $PV$  final states.

## B. Future Progresses in Describing Dalitz Plots

When LHCb and the B factories at SLAC and KEK was planned and approved CKM theory had a competition with other models for the leading source of CP violation in heavy flavour transitions. BaBar and Belle have found with great success that CKM provides at least the leading source of the establish CP asymmetries in  $B_d$  decays. LHCb is in a great position to find whether CKM is also the leading source of CP asymmetries in  $B_s$  decays even for  $B_s \rightarrow \psi\phi$  transitions that are largely reduced in CKM.

In addition LHCb and Super-Flavour Factories have to deal with the difficult task to find *non-leading* source(s) of CP asymmetries in suppressed decays. There are several candidates for that ND – even there is no ‘standard’ version of SUSY, let alone for other NDs.

The ‘Miranda Procedure’ can allow us to find a clean evidence for a CP asymmetry without a theoretical input. It will encourage much more theoretical progress on our understanding on soft QCD, which can make use of other theory tools obtained from hadronic dynamics. The tasks one faces in  $B$  and  $D$  decays into three-body final states are not quite as challenging as for the astronomers mentioned above: we know the locations where clear CP asymmetries can occur in  $B^0$  and  $D^0$  transitions – in particular in  $K_S\pi^+\pi^-$  and  $K_SK^+K^-$  final states: They get sizable contributions from  $K_S\rho^0$ ,  $K^{*\pm}\pi^\mp$  and  $K_S\phi$ . It has been shown that the Breit-Wigner parameterization provides a good approximation for vector mesons like  $\rho$ ,  $K^*$  and  $\phi$ . However scalar resonances will in general not be described that way; for a final state  $K_S f_0(980)$  it might give a decent description due to its relatively narrow width, but *not* for  $K_S\sigma(600)$  or  $\kappa\pi$  due to their wide widths. Still using a Breit-Wigner parametrization published data include true scalar resonances under ‘non-resonance’ label; more theoretical analyses including the treatment of chiral dynamics is needed, very topical – and possible now based on progress in the last few years. We know that they have to be performed *separately* for different  $B/D \rightarrow 3h$  transitions. We should understand the following: if present data for  $K\pi^+\pi^-$  final states are best fitted without any  $\sigma \rightarrow \pi^+\pi^-$  contribution or for two different  $\sigma_{1,2} \rightarrow \pi^+\pi^-$  one, one should not ignore one with the usual single  $\sigma(600)$  as long as it gives a satisfactory description. One needs more experimental and theoretical analysis.

There are several important reasons to analyze the production of scalar resonances in the detailed way. Let us just sketch one: Many models of ND contain physical charged Higgs states that can introduce CP asymmetries even through their *tree-level* exchanges. Obviously scalar Higgs exchanges will leave their ‘footprint’ in the production of scalar resonances with more weight than for pseudoscalar and vector states. Therefore such ND will produce more ‘readable’ impacts in CP asymmetries with scalar resonances and their interferences with pseudoscalar-vector final states. Therefore we can first focus on the known location of the peaks of the  $\rho$ ,  $K^*$  and the  $f_0(980)$  and their widths from available data. Using this general input from theory we can generate binning for  $B^0 \rightarrow K_S h^+ h^-$  and do it separately for  $B_d$  and  $B_s$  transitions.

## IV. SECOND GENERATION ‘MIRANDA PROCEDURE’

The procedure given in Ref. [13] is obviously powerful for finding CP asymmetries and even ‘localizing’ them. However one wants to make it more quantitatively and to understand its source(s) – in particular for  $B$  transitions CKM gives sizable ‘backgrounds’ when searching for ND.

The goal is to find a way to evaluate the strength of *local* effects, namely to have numbers that are equivalent to the asymmetry between (time) integrated rates,  $A_{CP}$ . The key idea is to divide the combined Dalitz plot into bins with equal populations. If one knows the number of bins where CP is violated, the one can compute a local average value of  $A_{CP}(s_1, s_2)$ , since the number of events is proportional to the number of bins.

Each bin has  $N = N^+ + N^-$  events, with  $N^+$  and  $N^-$  being the numbers of  $B$  and  $\bar{B}$  candidates. We assume that there are regions in the Dalitz plot with at least a few tens of bins in which positive events ( $N^+$ ) occur with the same

probability  $p$ .  $N^+$  follows a binomial distribution with expected value and variance given by

$$E[N^+] = Np, \quad V[N^+] = Np(1-p) \quad (52)$$

When  $N$  is large enough (at least a few tens of events), the Central Limit Theorem ensures that  $N^+$  follows a normal distribution, allowing one to write exact expressions for the expected difference  $N^+ - N^-$ . In this case one has

$$A_{\text{CP}}^{\text{bin}} = \frac{N^+ - N^-}{N} = \frac{2N^+}{N} - 1 \quad (53)$$

with

$$\mu = E[A_{\text{CP}}^{\text{bin}}] = \frac{2E[N^+]}{N} - 1 = 2p - 1 \quad (54)$$

and

$$\sigma^2 = V[A_{\text{CP}}^{\text{bin}}] = \frac{4V[N^+]}{N^2} = \frac{4p(1-p)}{N} \quad (55)$$

If CP symmetry is conserved – hereafter we assume that there is no other source of charge asymmetry – the probabilities of positive and negative events are equal,  $p = 1/2$ . One therefore has

$$\mu = 0, \quad \sigma^2 = \frac{1}{N} \quad (56)$$

When CP is violated the Dalitz plot will have regions with and *without* asymmetries. Therefore, the distribution of  $A_{\text{CP}}^{\text{bin}}$  will be a superposition of a Gaussian with  $\mu = 0$  and  $\sigma = 1/\sqrt{N}$  plus some other function representing the CP violating bins. The form of the latter depends on how CP violation occurs in the Dalitz plot and also on the specific final state.

Three-body final states result, in general, of a cascade process in which the heavy meson decays to a resonance plus a ‘bachelor’ hadron. The decay amplitude of a heavy meson  $P$  is usually modeled by a coherent sum of resonant amplitudes, weighted by constant complex coefficients

$$\mathcal{M} = \sum_i c_i A_i, \quad c_i = a_i e^{i\delta_i}. \quad (57)$$

CP violation results in a difference between  $\mathcal{M}(P)$  and  $\overline{\mathcal{M}} = \mathcal{M}(\overline{P})$ . More specifically,  $\mathcal{M}$  and  $\overline{\mathcal{M}}$  may

- differ by the *magnitude* of a set of resonant modes
- or a difference between their *relative phases*
- or a *combination* of both.

Rescattering at the hadronic level is a long distance effect that mixes different final states, e.g.  $\bar{K}K\pi \rightarrow \pi\pi\pi$ , and this is another source of CP violation.

In this paper, we consider three possibilities: (i) CP violation due to re-scattering as a constant excess of one specie over the other limited to some region of the Dalitz plot; (ii) CP violation through a difference in the magnitude of a resonant amplitude; (iii) a difference between relative phases.

The case of constant CP violation is the simplest: it leads to asymmetries that have always the same sign. An uniform and localized excess of one charge state over the other is equivalent to a constant value of  $p$ . In this case the distribution of CP violating bins will be a Gaussian with mean and sigma given by Eqs.(54) and (55). Integration over the phase space results is an observable global  $A_{\text{CP}}$ .

Differences in magnitude would also correspond, in principle, to a constant  $p$ . However, the net effect depends on the resonance spin and on the contribution of the other resonances. Angular momentum conservation constrains the angular distribution of the decay products. For vector particles, for example, the Breit-Wigner is modulated by a spin amplitude which is proportional to the cosine of an helicity angle. In the region where the momentum configuration is such that the helicity angle is  $90^\circ$ , the amplitude goes to zero. The relative contribution of the CP violating amplitude varies from bin to bin, in spite of the constant difference in its magnitude. Even in the case of a scalar resonance (constant spin amplitude), one needs to take into account the contribution from other resonant amplitudes to the CP violating bins, which in general is *not* constant. Also in this case an integration over the phase space results in an

observable global  $A_{\text{CP}}$ , although the local effect will be always diluted by the relative contribution of the CP violating amplitudes.

Differences in phases are the most complex case. As illustrated in [13], such differences lead to asymmetries that change sign across the Dalitz plot. Integration over the phase space could result in a null asymmetry, in spite of large local effects. In the simplest case of two resonances, Eq.(31) would read

$$A_{\text{CP}}(s_1, s_2) = \frac{2 \sin(\Delta\phi^W) \sin(\Delta\delta(s_1, s_2)) |\mathcal{A}_2 \mathcal{A}_1|}{1 + |\mathcal{A}_2 \mathcal{A}_1|^2 + 2 |\mathcal{A}_2 \mathcal{A}_1| \cos(\Delta\phi^W) \cos(\Delta\delta(s_1, s_2))} \quad (58)$$

The asymmetry is driven by  $\Delta\delta(s_1, s_2)$  due to interfering Breit-Wigner functions spread over the phase space. This is equivalent to having a different value of  $p$  for each bin. The distribution of  $A_{\text{CP}}^{\text{bin}}$  for the CP violating bins therefore depends strongly on the final state, on which resonances and with which relative phases it is built of.

An important effect is the charge asymmetry induced by different production mechanisms. This is not possible in  $p\bar{p}$  collider, but it may occur in asymmetric collisions (like for LHCb data). The production asymmetry may as large as a 1-2% effect. Since it depends on the heavy meson momentum, it may vary across the Dalitz plot. In the following examples we assume that any eventual production asymmetry would lead only to a global effect, constant throughout the Dalitz plot.

### A. Comment on CPT Constraints

It is mentioned usually that CPT symmetry gives equality of masses and total widths of  $P$  and  $\bar{P}$ . However it gives also equality of *different* classes of final states, where mixing happens; some general comments are given in Sect. 4.10 in [15]. Up to isospin violation one has for example:

$$\Gamma(B_{u,d,s} \rightarrow 2\pi, K\bar{K}, 4\pi, 2K2\bar{K}, 6\pi) = \Gamma(\bar{B}_{u,d,s} \rightarrow 2\pi, K\bar{K}, 4\pi, 2K2\bar{K}, 6\pi) \quad (59)$$

$$\Gamma(D_{u,d,s} \rightarrow 2\pi, K\bar{K}, 4\pi) = \Gamma(\bar{D}_{u,d,s} \rightarrow 2\pi, K\bar{K}, 4\pi) \quad (60)$$

While mixing happens – and diagrams show it – we have little *quantitative* control over it. In a qualitative way one expects correlations like between CP asymmetries in  $D^0 \rightarrow K^+K^-$  and  $D^0 \rightarrow \pi^+\pi^-$  or in  $\bar{B}_d \rightarrow K^-\pi^+$  and  $\bar{B}_d \rightarrow K_S\pi^0$  etc. As emphasized before that CP asymmetries with three-body final states will give us more information – and probably crucial one – about the underlying dynamics. Since SM produce sizable CP violation in  $b \rightarrow sq\bar{q}$  with  $q = u, d, s$  one expects sizable CP asymmetries in  $B_d \rightarrow K_S\rho^0/K_S\sigma/K^+\rho^-/\kappa\pi$  and higher resonances etc. with *different* signs compensate for CPT relation – but only qualitatively in practice.

### B. ‘Miranda Procedure’ for $B_d$ Three-Body Decays

We give ‘realistic’ studies for  $B_d \rightarrow K_S\pi^+\pi^-$ , where we have decent data and some information about the resonant structure [16, 17]. In all studies we consider time integrated, tagged samples. In each exercise two samples of  $B^0, \bar{B}^0 \rightarrow K_S\pi^+\pi^-$  were simulated independently using the same set of resonant amplitudes, namely  $K_S\rho, K_S f_0(980), K_S f_0(1370), K^*(892)\pi$  and  $K_S\chi_c$ . The samples are generated with CP violation seeded in three different ways, as described above.

A few remarks are in order:

- Indirect CP violation has been very well measured in  $B_d \rightarrow \psi K_S$  with  $\sin 2\phi_1/\beta = 0.658 \pm 0.024$ ; this observable enters in many transitions as an input quantity. However for the time integrated  $B_d + \bar{B}_d$  rates indirect CP asymmetry cannot contribute – *unless* there is a production asymmetry for  $B_d$  vs.  $\bar{B}_d$ .
- Direct CP violation can occur even in the time integrated  $B_d + \bar{B}_d$  rates.
- In the SM one has three quark-level processes, namely two tree-level  $b \rightarrow u\bar{u}s$  and  $b \rightarrow s\bar{u}u$ , where the second one is generated by QCD radiative corrections, and the loop Penguin  $b \rightarrow s + g's$ . They produce another  $\bar{d}d$  and  $\bar{u}u$  pair for the final state  $K_S\pi^+\pi^-$  and a  $\bar{s}s$  for  $B_d \rightarrow K_S K^+ K^-$ . The Penguin operator  $b \rightarrow s + g's$  generates no weak phase; since it produces a  $\Delta I = 0$  transition, there is no appreciable relative strong phase from this contribution. On the other hand  $b \rightarrow u\bar{u}s$  and  $b \rightarrow s\bar{u}u$  represent a combination of  $\Delta I = 0$  and  $\Delta I = 1$  amplitudes that in general will have different strong phases. As an example for ND: Charged Higgs exchanges would probably affect mostly  $b \rightarrow u\bar{u}s$  and  $b \rightarrow s\bar{u}u$ , introduce another weak phase and different strong phases. Furthermore they should affect final states with pseudoscalar-scalar more than pseudoscalar-vector. The impact of ND in direct CP violation should be clearer in the former than the latter, since the latter ‘suffer’ from a larger ‘background’ from CKM.

- Sizable contributions from final states  $K_S\rho$ ,  $K^*(892)\pi$ ,  $K^*(1430)\pi$ ,  $K_S f_0(980)$  and  $K_S f_0(1500)$  have been reported. No obvious contributions from  $K_S\sigma$  and/or  $\kappa\pi$  have been found, but might be hidden under the ‘no-resonance’ listing without 30 % of the rate of  $B_d \rightarrow K_S\pi^+\pi^-$ . There are several theoretical arguments that such final states  $K_S\sigma$  and  $\kappa\pi$  should occur in an appreciable way.
- While CKM dynamics has been found to produce at least the leading source of indirect CP violation in  $B_d - \bar{B}_d$  oscillations, ND could still represent up to about 20 % of it. While no clear deviation from CKM theory has been found in direct CP asymmetries in  $B_d$  decays, ND could produce significant contributions. One expects that the weight of ND in direct CP asymmetries will change differently for classes of channels like pseudoscalar-vector vs. pseudoscalar-scalar.

1.  $B_d/\bar{B}_d \rightarrow K_S\pi^+\pi^-$  – Constant CPV

Direct CP violation has been found in  $B_d \rightarrow K^+\pi^-$  around 10 %. No sign has been found in  $C(B_d \rightarrow K^0\pi^0) = 0.00 \pm 0.13$ . Yet one could find sizable impact with future data.

The first and simplest study of the ‘Miranda Procedure’ refers to the case where one has one single source of direct CP violation acting on a given region of the Dalitz plot. The CP violation is seeded as a 10% excess of  $B^0$  over  $\bar{B}^0$  in the region  $s_{K_S\pi^+}, s_{\pi^+\pi^-} < 7.5 \text{ GeV}^2/c^4$ . We have generated 300K  $B^0$  and 330K  $\bar{B}^0$  decays dividing the combined Dalitz plot into 256 bins of equal population. This excess of  $B^0$  over  $\bar{B}^0$  events is equivalent to a global  $A_{CP}$  of 4.76%. The distribution of the  $A_{CP}^{\text{bin}}$  across the Dalitz plot is shown in Fig.1.

Having only one source of CP violation (constant  $p$ ), the values of  $A_{CP}^{\text{bin}}$  for the bins in the region where CP violation was seeded are the same within statistical fluctuations. We therefore expect the  $A_{CP}^{\text{bin}}$  for the CP violating bins to be also distributed as a Gaussian. The distribution in Fig.2 is fitted by two Gaussian functions. The one representing the CP conserving bins has fixed mean ( $\mu = 0$ ) and sigma ( $\sigma = 1/\sqrt{N}$ ), whereas the parameters defining the second Gaussian are free.

The average value of  $A_{CP}^{\text{bin}}$  in the region where CP violation was seeded is the mean of the second Gaussian,  $(13.64 \pm 0.25)\%$ . The normalization of each Gaussian is the number of bins that conserve/violate CP. There are  $167 \pm 13$  bins conserving CP and  $89 \pm 9$  bins in which CP is violated. The number of events is the same for all bins, so we can obtain the global  $A_{CP}$  from the ratio of CP violating to the total number of bins, and from the average value of  $A_{CP}^{\text{bin}}$ ,

$$A_{CP} = \frac{n_2}{n_1 + n_2} < A_{CP}^{\text{bin}} > = 4.98 \pm 0.54\% \quad (61)$$

We not only recover the global  $A_{CP}$  but also access the average  $A_{CP}^{\text{bin}}$  and the fraction of events that violate CP and thus the localization of the source.

This exercise clearly shows how the relatively large local effect is diluted when the CP violation strength is measured by the global  $A_{CP}$  (in this case, by the ratio of the area of the CP violation region and the total Dalitz plot area).

2.  $B_d/\bar{B}_d \rightarrow K_S\pi^+\pi^-$  – Difference in Magnitudes

In this example CP violation is seeded as a 10% difference in the magnitude of the resonant mode  $K^*(892)\pi$ ,  $a_{K^*(892)\pi} = 0.9\bar{a}_{K^*(892)\pi}$ .

The total decay rates of  $B^0$  and  $\bar{B}^0$  are proportional to the integral over the phase space of  $\mathcal{M}$  and  $\bar{\mathcal{M}}$ , respectively. In the present example, this means a global CP asymmetry of 2.1%. Samples of 300K  $B^0$  and 287K  $\bar{B}^0$  decays were generated. The combined  $B^0$  and  $\bar{B}^0$  Dalitz plot was divided into 1024 bins of equal population.

The extra  $B^0$  events are distributed in the bins along the  $K^*(892)$  band, and the resulting  $A_{CP}^{\text{bin}}$  across the Dalitz plot is shown in Fig.3; note that the values of  $A_{CP}^{\text{bin}}$  in the CP violating region are always positive.

In Fig.4 the distribution of  $A_{CP}^{\text{bin}}$  for all bins is presented. The bins with no CP violation have equal number of  $B^0$  and  $\bar{B}^0$  decays, within statistical fluctuations, resulting on a Gaussian distribution of  $A_{CP}^{\text{bin}}$  with  $\mu = 0$  and  $\sigma = 1/\sqrt{N}$ . The distribution of  $A_{CP}^{\text{bin}}$  for the CP violating bins is again parameterized by Gaussian, but this is used as an effective representation ( $p$  is no longer constant). As in the previous example, the distribution in Fig.4 is fitted to two Gaussian functions, one with fixed mean and sigma representing the CP conserving bins.

We find  $838 \pm 46$  bins with no CP violation and  $186 \pm 38$  bins with average value of  $A_{CP}^{\text{bin}}$   $(11.1 \pm 1.7)\%$ . From these parameters we extract the global asymmetry,  $A_{CP} = 2.1 \pm 0.1\%$ .

These exercises show that the observable  $A_{CP}^{\text{bin}}$  carries the relevant information about local asymmetry. In both cases the CP violation is restricted to certain regions of the Dalitz plot, but leads to a global asymmetry. The local

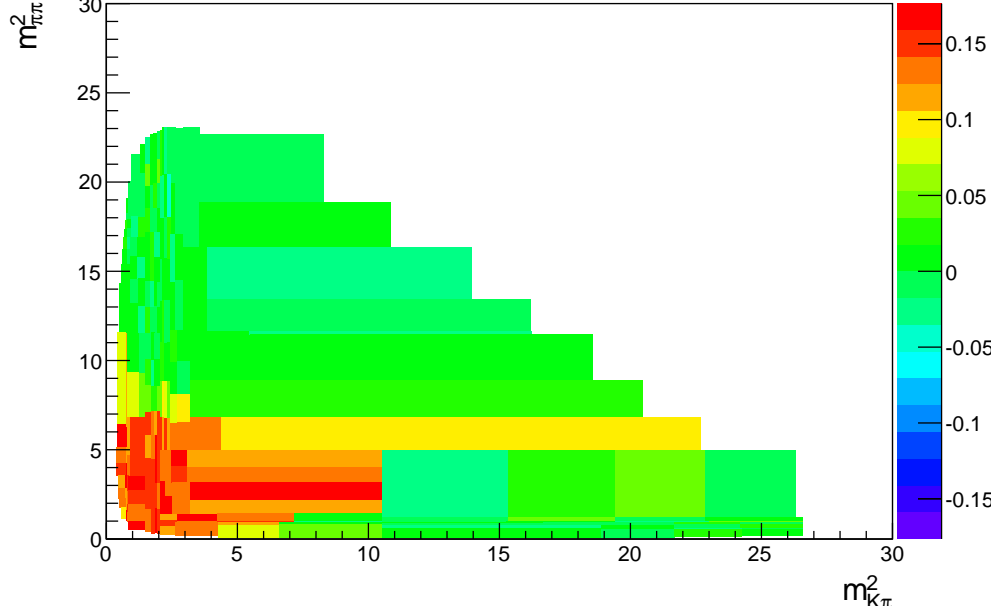


FIG. 1. Distribution of  $A_{\text{CP}}^{\text{bin}}$  across the  $B_d \rightarrow K_S \pi^+ \pi^-$  Dalitz plot. In this example a single source of CP violation – constant excess of  $B_d$  over  $\bar{B}_d$  restricted to the low  $K_S \pi^+ / \pi^+ \pi^-$  mass region – was simulated. Bins have different size in order to contain the same number of events.

effects are much more intense than the phase space integrated ones. We showed that the later can be recovered in a consistent way.

### 3. $B_d/\bar{B}_d \rightarrow K_S \pi^+ \pi^-$ – Difference in Relative Phases

We now discuss a more general case, where the CP violation occur via a difference between  $B$  and  $\bar{B}$  in relative phase of a given set of resonances. This is a much more difficult and subtle situation, which depends strongly on the final state characteristics: (i) Which resonances are present. (ii) What are their relative phases. (iii) Is there an sizable contribution from scalars [18].

Two independent samples were generated using the same set of resonances as in the previous examples. A  $60^\circ$  phase difference in the  $\rho K_S$  mode was introduced between  $B_d$  and  $\bar{B}_d$ . The combined Dalitz plot was then divided into 1024 bins. The seeded phase difference is large, causing local asymmetries that can be as large as 80%, shown in Fig.5. The *global* asymmetry, however, is small: 1.0%. Due to the phase variation of the Breit-Wigner curve, the CP asymmetry change sign along the  $\rho$  band. In this case the integration over the phase space – necessary to compute the total rates – cancels out most of the effect of CP violation. This cancellation is clearly seen in Fig.6, which has an enlarged view of the Dalitz plot region where CP violation occur.

The interference between  $\rho K_S$  and the other resonant modes, which is governed by the combined strong phases of the Breit-Wigner curve,  $\Delta\delta(s_1, s_2)$ , causes each bin to act as an independent source of CP violation. When one has repeated the same experiment many times, the values of  $A_{\text{CP}}^{\text{bin}}$  for each bin would be distributed with a mean and sigma given by Eqs.(54,55), respectively, each bin having its own value of  $p$ . The distribution of  $A_{\text{CP}}^{\text{bin}}$  for all bins will have two components, as in the other examples. The distribution from the CP violating bins would no longer be a Gaussian, but some function that is particular to each specific final state.

In general there would be as many bins with *positive* and *negative*  $A_{\text{CP}\pm}^{\text{bin}}$ , so the procedure adopted in the previous examples would underestimate the measurement of the average asymmetry in this case. As before, we can fit the distribution to a Gaussian for the CP conserving bins –  $\mu = 0$  and  $\sigma = 1/\sqrt{N}$ , but with unknown area – plus one function for the CP violating bins. Having defined the Gaussian CP conserving bins, this can then be subtracted off, and two numbers could be computed: the average value of  $A_{\text{CP}\pm}^{\text{bin}}$  for the regions where the asymmetry is either positive or negative.

We illustrate this procedure in Fig.7, where the  $A_{\text{CP}}^{\text{bin}}$  distribution for the CP violating bins was empirically fit to two Gaussians. The fit yields  $568 \pm 83$  bins in the CP conserving Gaussian, and  $466 \pm 41$  bins in which CP is violated.



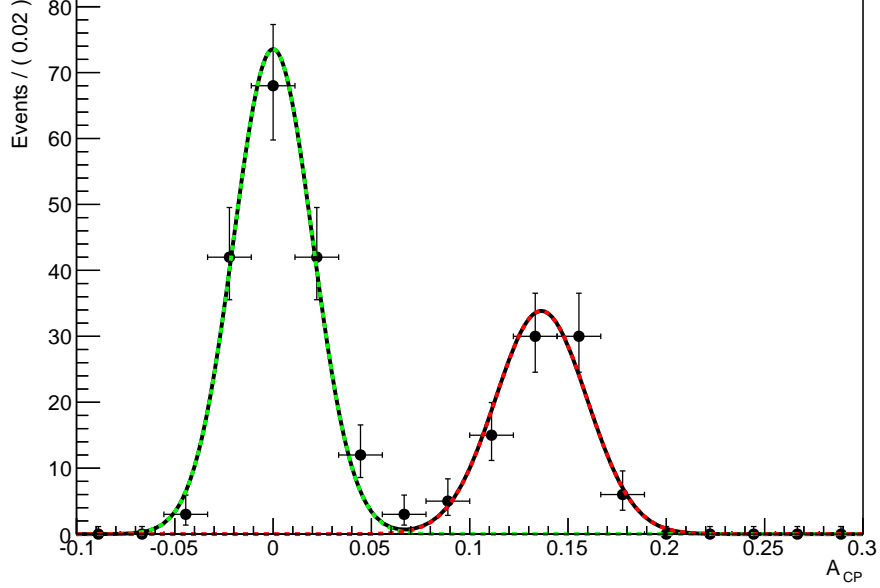


FIG. 2. Distribution of  $A_{CP}^{\text{bin}}$  for single, constant source of CP violation. The distribution was fitted to two Gaussians. The one centered at zero represents bins where CP is conserved, whereas the second Gaussian represents the CP violating bins.

We then compute the weighted average value of  $A_{CP\mp}^{\text{bin}}$  for the negative and for the positive part of the distribution in Fig.7. This yields

$$\langle A_{CP-}^{\text{bin}} \rangle = -(14 \pm 2)\%, \quad (62)$$

and

$$\langle A_{CP+}^{\text{bin}} \rangle = (16 \pm 2)\%. \quad (63)$$

In order to test this procedure, we go to the limit of very high statistics. Since the width of the distribution of CP conserving bins is  $\sigma = 1/\sqrt{N}$ , when  $N$  is very large, the Gaussian gets very narrow, in practice restricted to the central bin of Fig.7. We can then compute the weighted average in the negative and positive regions separately with a simple counting procedure, discarding the central bin. The average values of  $A_{CP\mp}^{\text{bin}}$  obtained are

$$\langle A_{CP-}^{\text{bin}} \rangle = -15\% \quad (64)$$

and

$$\langle A_{CP+}^{\text{bin}} \rangle = 22.2\% \quad (65)$$

in good agreement with the fitting procedure used in the more realistic scenario.

## V. $B_s$ THREE-BODY DECAYS

At present, the experimental situation is very different for  $B_s$  transitions even beyond the fact that  $B_s - \bar{B}_s$  oscillations are very fast.

- Within SM indirect CP violation is small – i.e.  $\sin 2\beta_s \sim 0.03 - 0.05$ . Finding it significantly larger is a clear manifestation of ND. There is some evidence that indirect CP violation is larger than predicted by CKM; studies of  $B_s \rightarrow \psi\phi$  in LHC data should clarify this issue and allow  $\sin 2\beta_s$  as an input for searching manifestations of ND.
- If one indeed finds that CKM theory does not produce the leading source of indirect CP violation, there is a good chance that ND generates a larger contribution also to direct CP violations.

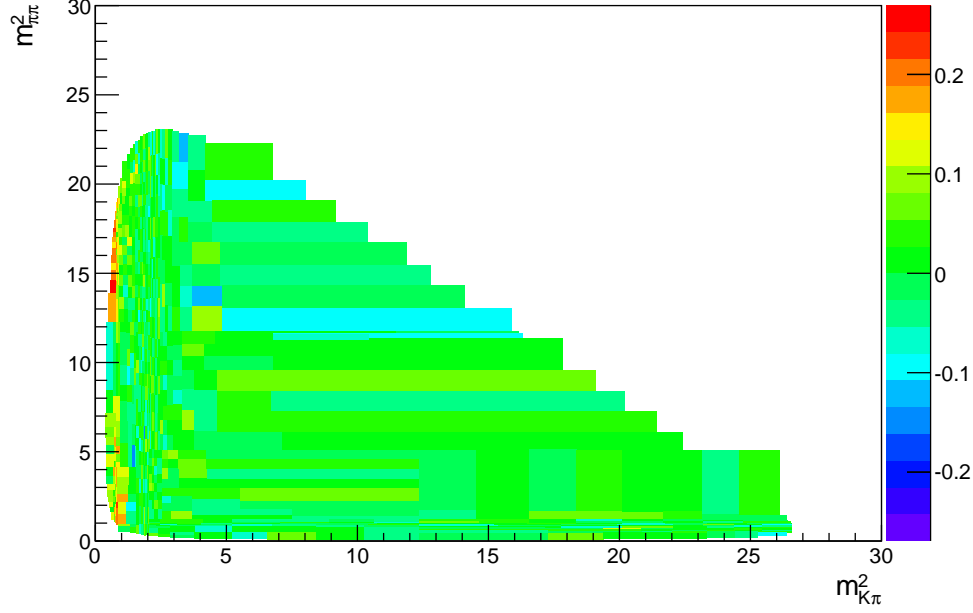


FIG. 3. Distribution of  $A_{\text{CP}}^{\text{bin}}$  across the  $B_d \rightarrow K_S \pi^+ \pi^-$  Dalitz plot for the case of CP violation seeded as a difference in the magnitude of the  $\rho K_S$  mode between  $B_d$  and  $\bar{B}_d$ . The excess of  $B_d$  over  $\bar{B}_d$  events is concentrated along the  $\rho$  band. Note that the values of  $A_{\text{CP}}^{\text{bin}}$  for these bins are always positive.

- Measuring  $y_s$  more accurately will help in cross checking finding CP asymmetries in the sum of time integrated  $B_s$  and  $\bar{B}_s$  rates.
- There are no data for  $B_s \rightarrow K_S \pi^+ \pi^-$  or  $B_s \rightarrow K_S K^+ K^-$ . One expects the Dalitz plots for these  $B_s$  transitions very different for these  $B_d$  transitions.
- The tree diagram  $b \rightarrow u\bar{u}d$  and the Cabibbo disfavoured penguin one-loop diagram  $b \rightarrow d + g's$  to generate direct CP violation in both CKM and ND. Again final states like  $K_S \sigma$  should show clearly manifestations of the impact of ND.

## VI. OUTLOOK

Present data from Belle, BaBar, CDF and LHCb and future ones from LHCb, Super-Belle and Super-BaBar have reached the status to probe the possible impact from ND in  $B_{u,d,s}$  and  $D_{u,d,s}$  with *accuracy* and *correlations*. Analyzing non-leptonic three-body final states there needs significantly more experimental efforts through ‘Miranda Procedure’ – but it will be awarded with more lessons about the underlying dynamics and deep insights into its ‘shape’.

The *Miranda Procedure I* is a good way to show whether or not there is CP asymmetry in three-body decays of  $D$  and  $B$  mesons. It can also tell us where in the Dalitz plot CP violation occurs and give hints of the kind of operators that are involved. A further development of this technique, presented here, is a necessary step towards a quantitative output. One should keep in mind, however, the crucial difference between two- and three-body decays: while in former case CP asymmetries are observed in total decay rates, in the latter case there are several options for CP violation manifestations. CP asymmetries through phase difference – ‘favorited’ by model builders – are intrinsically complicated because each bin acts as an independent source of CPV. Moreover, strong interactions governing phases across the Dalitz plot are still out of control *quantitatively*. Accurate data on three-body final states will help efforts from theorists working on HEP and Hadrodynamics/MEP.

One should not forget about constraints from CPT symmetry, but those are not of *quantitative* value on a practical level; it should tell us to think about other channels in a qualitative level; theoretical inputs help here.

The ‘Miranda Procedure’ helps greatly to ‘localize’ CP asymmetries and find evidence for the impact of ND and its ‘shape’. It does not mean that theoretical inputs are not needed, but to focus on them. It should enhance interests from theorists working in HEP and HP/MEP.

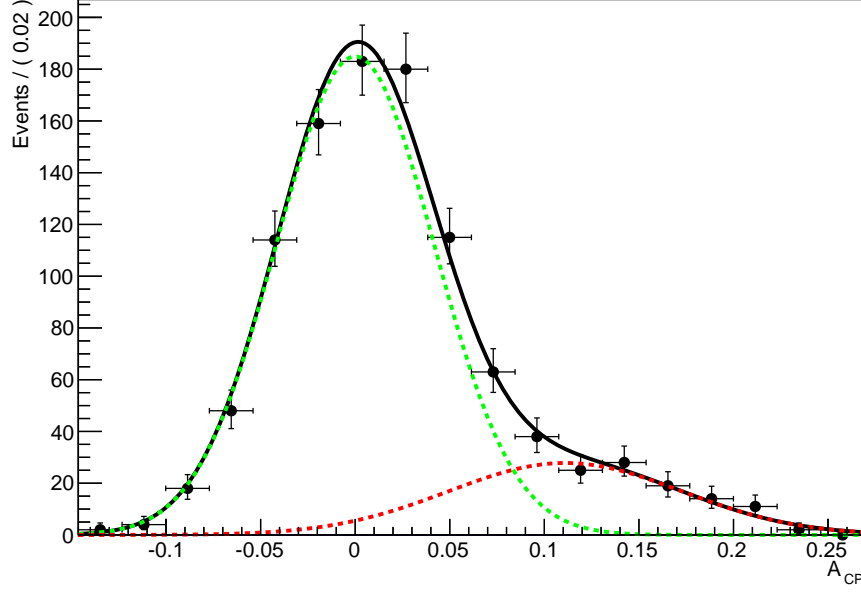


FIG. 4. Distribution of  $A_{\text{CP}}^{\text{bin}}$  for the case of CP violation through a difference in the magnitude of the  $\rho K_S$  mode. The Gaussian in red is an empirical representation of  $A_{\text{CP}}^{\text{bin}}$  for the CP violating bins.

Applying ‘Second Generation of Miranda Procedure’ is now at the ‘starting line’ – the ‘race’ will proceed over many longer ‘distances’ with simulations and – most importantly – with real data:

- Time integrated and non-flavour tagged rates for  $B_{u,s}/D_{u,d,s}$  decays;
- Flavour tagged ones for  $B_{u,d,s}/D_{u,d,s}$ ;
- partially time integrated ones;
- $\tau \rightarrow \nu[K\pi/K2\pi/3K]$  decays.

One needs no more hardware – ‘only’ thinking and working.

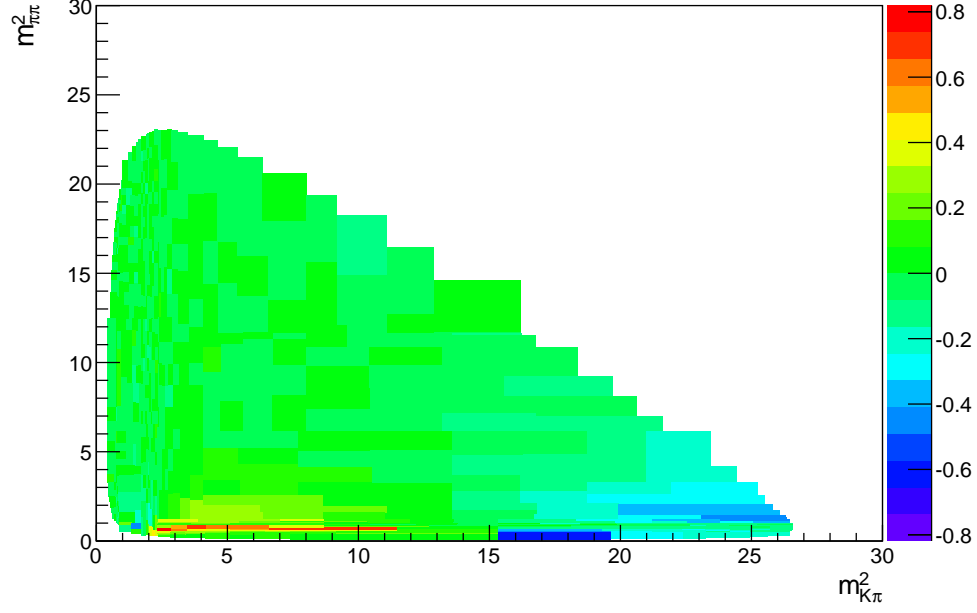


FIG. 5. Distribution of  $A_{\text{CP}}^{\text{bin}}$  across the  $B_d \rightarrow K_S \pi^+ \pi^-$  Dalitz plot for the third example. When the CP violation is seeded as a relative phase difference, the values of  $A_{\text{CP}}^{\text{bin}}$  change sign.

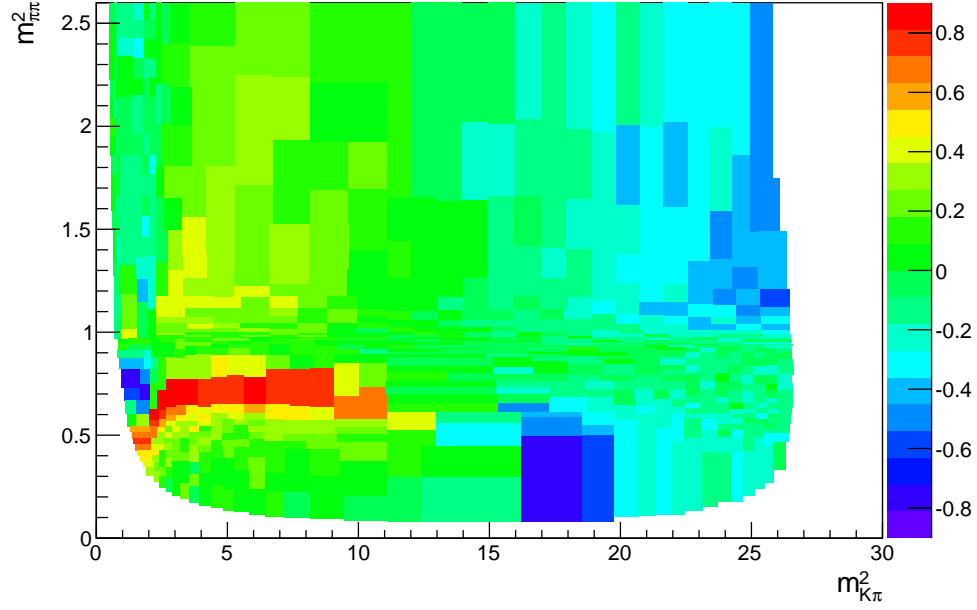


FIG. 6. Enlarged view of the CP violating bins of Fig.5.

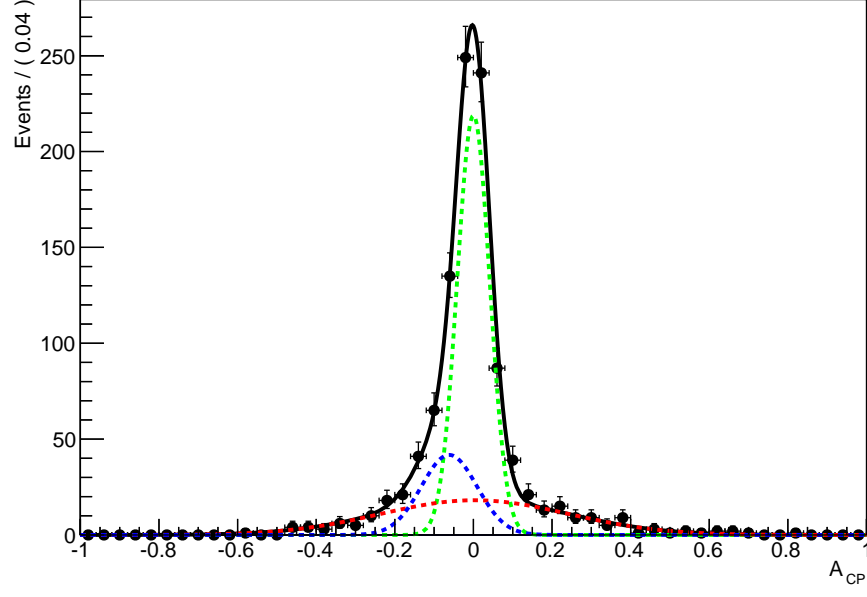


FIG. 7. Distribution of  $A_{CP}^{\text{bin}}$  for the third example. In addition to the Gaussian representing the CP conserving bins (green curve), two other Gaussians were used to empirically represent the  $A_{CP}^{\text{bin}}$  distribution of the CP violating bins (red and blue curves).

**Acknowledgments:** This work was supported by the NSF under the grant number PHY-0807959 and by CNPq.

- 
- [1] The Review of Particle Physics. K. Nakamura *et al.* (Particle Data Group), J. Phys. G 37, 075021 (2010).
  - [2] The LHCb Collaboration, R. Aaij *et al.*, Phys. Rev. Lett. 108, 101803 (2012), Phys. Lett. B707 (2012)
  - [3] The LHCb Collaboration, R. Aaij *et al.*, arXiv:1202.6251v1 [hep-ex].
  - [4] The CDF Collaboration, T. Aaltonen *et al.*, Phys. Rev. Lett. 106, 181802 (2011).
  - [5] <http://www.slac.stanford.edu/xorg/hfag/>
  - [6] R. Aaij *et al.*, LHCb Collaboration, Phys. Rev. Lett. 108 (2012) 111602
  - [7] The CDF Collab., CDF Note 10784.
  - [8] I. I. Bigi, A.I. Sanda, *Phys.Lett.* **B625** (2005) 47; arXiv:hep-ph/0506037; Y. Grossman and Y. Nir, arXiv:1110.3790 [hep-ph] (2011) finding a sign mistake in intermediate transitions in the paper by Bigi & Sanda, but came up with the same final CP asymmetry; the authors of the first paper had used the definition of ‘Bavarian Illuminati’ of  $|q|$  and  $|p|$ .
  - [9] The BaBar Collaboration, J. P. Lees *et al.*, arXiv:1109.1527v2[hep-ex].
  - [10] Y.H. Ahn, H-Y. Cheng, S. Oh, arXiv:1106.0935v2[hep-ph].
  - [11] I.I. Bigi, A. Paul, to appear very soon.
  - [12] I.I. Bigi, arXiv:1204.5817[hep-ph].
  - [13] I. Bediaga *et al.*, Phys.Rev.**D80**(2009)096006; arXiv:0905.4233[hep-ph].
  - [14] M.Williams, Phys.Rev.**D84** (2011) 054015.
  - [15] For a very recent review see: I.I. Bigi, A.I. Sanda, ”CP Violation, Second Edition”, *Cambridge Monographs on Particle Physics, Nuclear Physics and Cosmology* (Cambridge University Press) 2009.
  - [16] The BaBar Collaboration, B. Aubert *et al.*, Phys.Rev.**D80** (2009) 112001.
  - [17] The Belle Collaboration, J. Dalseno *et al.*, Phys.Rev.**D79** (2009) 072004.
  - [18] Analyzing Dalitz plots with different phases needs much more efforts on the experimental side – and the theoretical side even more. One of us sees this obvious challenge as a job opportunity for young theorists, since most of the tools exist from Middle Energy Physics – like dispersion relations – it ‘just’ needs more work.